Published in final edited form as:

Neuron. 2016 August 3; 91(3): 629–643. doi:10.1016/j.neuron.2016.06.032.

Multimodal and site-specific plasticity of amygdala parvalbumin interneurons after fear learning

Elizabeth K. Lucas[1], **Anita M. Jegarl**[1], **Hirofumi Morishita**[1,2], and **Roger L. Clem**[1,2]

[1]Fishberg Department of Neuroscience and the Friedman Brain Institute, Icahn School of Medicine at Mount Sinai, New York, NY, USA

[2]Department of Psychiatry and the Friedman Brain Institute, Icahn School of Medicine at Mount Sinai, New York, NY, USA

Summary

Stimulus processing in fear conditioning is constrained by parvalbumin-interneurons (PV-INs) through inhibition of principal excitatory neurons. However, the contributions of PV-IN microcircuits to input gating and long-term plasticity in the fear system remain unknown. Here we interrogate synaptic connections between afferent pathways, PV-INs, and principal excitatory neurons in the basolateral amygdala. We find that this region is populated by at least two functionally distinct PV-IN networks based on nucleus location. PV-INs in the lateral (LA), but not the basal (BA), amygdala possess complex dendritic arborizations, receive potent excitatory drive, and mediate feedforward inhibition onto principal neurons. After fear conditioning, PV-INs exhibit nucleus- and target-selective plasticity, resulting in persistent reduction of their excitatory input and inhibitory output in LA but not BA. These data reveal previously overlooked specializations of PV-INs within amygdala subnuclei and indicate specific circuit mechanisms for inhibitory plasticity during the encoding of associative fear memories.

Introduction

Aversive memories acquired by classical conditioning provide insight into emotional learning under normal conditions as well as pathological states, such as posttraumatic stress disorder (PTSD; Mahan and Ressler, 2012). Cellular models of fear learning place a great deal of emphasis on amygdala excitatory neuronal plasticity (Janak and Tye, 2015; Johansen et al., 2011). However, many studies posit that co-regulation of excitation and inhibition may be important for network stability and that excitation:inhibition (E:I) imbalance may be a

*Corresponding author: Roger L. Clem, One Gustave L. Levy Place, Box 1065, New York, NY 10029, roger.clem@mssm.edu, Phone: (212) 824-8976, Fax: (212) 849-2611.

Author Contributions. Conceptualization, E.K.L. and R.L.C.; Methodology, E.K.L. and R.L.C.; Investigation, E.K.L., A.M.J., and R.L.C.; Writing – Original Draft, E.K.L. and R.L.C.; Writing – Review & Editing, E.K.L., A.M.J., H.M., and R.L.C.; Funding Acquisition, E.K.L. and R.L.C.; Resources, H.M. and R.L.C.; Supervision, E.K.L and R.L.C.

The authors declare no conflicts of interest.

factor in some psychiatric conditions (Dorrn et al., 2010; Gouty-Colomer et al., 2015; House et al., 2011; Katagiri et al., 2007; Vogels et al., 2011). Notably, decreased GABA levels as well as GABA receptor binding and polymorphisms have been associated with PTSD (Bremner et al., 2000; Feusner et al., 2001; Geuze et al., 2008; Meyerhoff et al., 2014; Pennington et al., 2014; Rossi et al., 2009; Rosso et al., 2014), and reduced GABA levels are predictive of disease progression (Vaiva et al., 2006; Vaiva et al., 2004). Changes in inhibitory synaptic markers suggest that plasticity of GABAergic transmission in the basolateral amygdala may also be a feature of aversive memory formation under normal conditions (Chhatwal et al., 2005; Heldt and Ressler, 2007; Lin et al., 2011). Although *ex vivo* stimulation of amygdala brain slices has been shown to induce long-term plasticity in undefined GABAergic populations (Bauer and LeDoux, 2004; Mahanty and Sah, 1998; Polepalli et al., 2010; Shin et al., 2006; Szinyei et al., 2000), it remains unknown whether specific GABAergic cell types exhibit plasticity associated with emotional learning.

The majority of GABAergic synaptic inhibition throughout the forebrain is thought to originate from a heterogeneous population of locally-projecting interneurons. Within the basolateral amygdala, more than half of inhibitory synapses formed onto principal excitatory neurons are associated with PV-INs (Muller et al., 2006), which are considered to exert powerful control over the firing of these cells through dense somatic and axo-axonic synaptic terminals (Hu et al., 2014). Recently, *in vivo* manipulations within the basolateral amygdala (Wolff et al., 2014) as well as neocortical regions (Courtin et al., 2014; Letzkus et al., 2011) have implicated PV-INs in fear acquisition and expression through cue-related inhibition and disinhibition of principal excitatory neurons. Therefore, it is important to understand the circuit mechanisms underlying PV-IN recruitment and resulting excitatory neuronal inhibition as well as to determine whether fear conditioning generates persistent alterations in PV-IN function.

We utilized parvalbumin-specific Cre driver mice as well as optogenetic-assisted electrophysiology to investigate the properties and experience-dependent plasticity of PV-IN microcircuits. We report that function and plasticity of PV-INs varies by nucleus location within basolateral amygdala and that fear conditioning leads to downregulation of PV-IN transmission predominantly within microcircuits that mediate feedforward inhibition from sensory afferent pathways.

Results

Uniquely Robust Afferent Excitation of Lateral Amygdala PV-INs

To selectively target PV-INs for *in vitro* electrophysiology, we crossed R26-STOP-eYFP reporter mice to the PV-IRES-Cre driver line to selectively express enhanced yellow fluorescent protein (eYFP) in PV-INs. Given a previous report that only ~60% of PV-positive cells in the basolateral amygdala co-express GABA (McDonald and Mascagni, 2001), we sought to determine the specificity of Cre-mediated recombination by quantifying double immunofluorescence staining with antibodies against parvalbumin and GABA (Figure 1A, Figure S1). More than 90% of eYFP-positive cells in the basolateral amygdala co-expressed both PV and GABA (Figure S1), demonstrating that this Cre line is highly selective for GABAergic PV-INs in this brain region.

During classical conditioning, a benign auditory conditioned stimulus (CS) is paired with a naturally aversive unconditioned stimulus (US), forming an associative memory that links the CS and US. *In vivo* studies have found that amygdala PV-INs respond differentially to sensory stimulation with increased firing to auditory stimuli (Wolff et al., 2014) and decreased firing to footshock (Wolff et al., 2014) and other noxious stimuli (Bienvenu et al., 2012). However, it is unknown whether PV-INs are directly modulated by afferent pathways conveying CS activity. To address this question, we performed whole-cell recordings from PV-INs and neighboring principal neurons during stimulation of subcortical and cortical sensory afferent pathways, which traverse the internal and external capsules, respectively. We first investigated the input/output (I/O) relationship of compound postsynaptic currents consisting of monosynaptic excitatory postsynaptic currents (EPSCs) and disynaptic feedforward inhibitory postsynaptic currents (IPSCs) at increasing stimulus intensities (Figure 1B–K). While there was no difference in the I/O slope of IPSCs between populations, the I/O relation of monosynaptic EPSCs from both subcortical and cortical afferents was far steeper in LA PV-INs compared to their glutamatergic neighbors (Figure 1G; two-way ANOVA, main effect of neuron type, $F_{(1,22)} = 30.89$, $p < 0.0001$), indicating far greater excitatory drive from these pathways in PV-INs. While converging excitation from the subcortical and cortical pathways to the LA is hypothesized to be a key mediator of learning-induced synaptic plasticity (Sigurdsson et al., 2007), cortical neurons also send axon collaterals to BA (Sah et al., 2003; Turner and Herkenham, 1991). To determine whether these inputs exhibit similar potency, we investigated the I/O relationship of BA cortical synaptic currents (Figure 1H–K). Unlike in LA, PV-INs and PNs in BA exhibited similar I/O slope of both monosynaptic EPSCs and feedforward IPSCs (Figure 1K). We then calculated an index of I/O slopes (calculated as I/O slope_{EPSC}/ I/O slope_{IPSC}) as a measure of E:I balance for LA and BA neurons. PV-INs in LA exhibited greater E:I index compared to PV-INs in BA as well as to principal neurons in both nuclei (Figure 1L; two-way ANOVA, main effect of neuron type, $F_{(1,33)} = 27.13$, $p < 0.0001$; main effect of nucleus, $F_{(2,33)} = 3.76$, $p = 0.03$; interaction, $F_{(2,33)} = 6.47$, $p = 0.004$). Importantly, EPSC onset latency was similar across cells and nuclei (Figure 1M), indicating that these responses shared a monosynaptic mechanism.

To determine whether differences in PV-IN anatomy could account for nucleus-specific excitatory drive, we performed morphological reconstructions of biocytin-filled PV-INs (Figure 1N). While soma and primary dendrite characteristics were comparable between nuclei, PV-INs in LA possessed twice as many dendritic branches ($t_{(18)} = 3.09$, $p = 0.006$) as those in BA, resulting in increased dendritic length ($t_{(18)} = 2.27$, $p = 0.04$; Figure 1O). Furthermore, truncated dendrites were very infrequent and the total number of such artifacts was similar between nuclei (LA = 4; BA = 3), indicating that the observed differences in physiology and morphology were not attributable to slice preparation.

PV-INs Meditate Feedforward Inhibition in Lateral but not Basal Amygdala

Given the potent excitatory drive onto LA PV-INs, we hypothesized that PV-INs may generate greater feedforward inhibition onto principal neurons in LA compared to BA. To test this hypothesis, we harnessed the power of optogenetics to silence PV-INs during afferent stimulation while recording feedforward IPSCs. Conditional expression of the GFP-

tagged enhanced light-driven inhibitory proton pump Archaerhodopsin-3.0 (eArch3.0; Chow et al., 2010) in PV-IRES-Cre mice resulted in GFP expression in both the soma and axonal arbors of PV-INs (Figure S2A–B). Whole-cell recordings in eArch3.0-expressing cells confirmed yellow light-induced (λ = 590 nm) neuronal silencing (Figure S2C–E). Notably, PV-INs escaped voltage clamp and generated rebound action currents following light offset at every stimulus intensity (Figure S2C).

To evoke monosynaptic EPSCs and feedforward IPSCs, principal neurons were clamped at membrane potentials of −70 mV and 0 mV, respectively, during stimulation of subcortical and cortical afferents. Feedforward IPSCs were abolished by the $GABA_A$ receptor antagonist picrotoxin as well as the AMPA/kainate receptor antagonist CNQX (Figure 2B). In addition, the onset latency of feedforward IPSCs was delayed relative to EPSCs (independent samples t-test, $t_{(36)} = 11.01$, $p < 0.0001$), consistent with a disynaptic circuit mechanism (Figure 2C).

Having validated our approach, we patched onto principal neurons in mice with conditional eArch3.0 expression in PV-INs and recorded feedforward IPSCs evoked by subcortical or cortical afferent stimulation in the presence or absence of yellow light (Figure 2A). Feedforward IPSCs from both pathways were attenuated by silencing PV-INs in LA (Figure 2D–G; paired samples t-test, subcortical: $t_{(13)}= 3.59$, $p = 0.003$, cortical: $t_{(7)} = 2.57$, $p = 0.03$). Consistent with low cortical excitatory drive onto BA PV-INs (Figure 1L), PV-IN silencing did not affect the amplitude of feedforward IPSCs in this nucleus (Figure 2I–J; paired samples t-test, $t_{(11)} = 0.05$, $p = 0.96$).

Consistent with our observation of rebound action currents in eArch3.0-expressing cells (Figure S2C), we also observed corresponding rebound IPSCs in principal neurons at LED offset (Figure 2E,G,J). Interestingly, we found that peak rebound amplitude positively correlated with reduction of feedforward IPSC amplitude by LED illumination (Figure 2H; linear regression, $F_{(1,20)} = 29.09$, $p < 0.0001$). Since rebound amplitude partly reflects the number of viable eArch3.0-infected PV-INs in our recording field, this further indicates that PV-INs are readily engaged in feedforward inhibition in the LA.

Fear Conditioning Induces Nucleus-Specific Alterations in PV-IN Synaptic Input

To determine whether fear learning alters PV-IN properties, we conducted whole-cell recordings in PV-INs after auditory fear conditioning, which entailed paired or unpaired presentations of an auditory tone (CS) and footshock (US). We confirmed that auditory fear was specific to the paired condition, since CS-evoked freezing was observed 24 hours later in mice that received paired but not unpaired training (Figure S3). All electrophysiological recordings were obtained 24 hours after training from a different set of animals in which retrieval was omitted in order to exclude the possibility of memory extinction or reconsolidation. An analysis of miniature (m) EPSCs and mIPSCs from paired, unpaired, and naïve mice at this time point revealed nucleus-specific alterations in PV-INs that were correlated with auditory fear encoding (Figure 3). The frequency of mEPSCs differed between conditions in LA (one-way ANOVA, $F_{(2,22)} = 3.78$, $p = 0.04$) but not in BA (one-way ANOVA, $F_{(2,33)} = 2.34$, $p = 0.11$; Figure 3B–D, I–K). In LA PV-INs, mEPSC frequency was reduced in paired ($p = 0.008$), but not in unpaired ($p = 0.74$), mice compared to naïve

controls. In contrast, the frequency of mIPSCs differed between conditions in BA (one-way ANOVA, $F_{(2,32)} = 4.42$, $p = 0.02$) but not in LA (one-way ANOVA, $F_{(2,22)} = 0.31$, $p = 0.74$;Figure 3E–G, L–N). In BA PV-INs, mIPSC frequency was increased in paired ($p = 0.03$), but not unpaired ($p = 0.48$), mice relative to naïve controls. Fear conditioning did not affect the amplitude or kinetics of mEPSCs or mIPSCs. However, independent of fear conditioning, these properties were strongly affected by nucleus location of PV-INs (Figure S4).

The above changes suggest that PV-INs are modulated by a nucleus-specific adjustment of their presynaptic input. Given robust excitation of PV-INs by amygdala afferents (Figure 1), we questioned whether excitatory presynaptic plasticity could be attributed to these pathways. As an assay of glutamate release probability, we measured the paired pulse ratio (PPR) of EPSCs evoked by subcortical and cortical stimulation. Consistent with decreased release probability, PPR was increased at both subcortical (repeated-measures ANOVA, main effect of group, $F_{(2,72)} = 26.23$, $p < 0.001$) and cortical synapses (repeated-measures ANOVA, main effect of group, $F_{(2,104)} = 41.73$, $p < 0.001$) in LA of mice that received paired training compared to unpaired and naïve controls (Figure 4A–F). Interestingly, PPR was also decreased at cortical synapses after unpaired training (Figure 4E), but evidently this was not sufficient to enhance overall excitation onto LA PV-INs (Figure 3B). To determine whether presynaptic plasticity was nucleus-specific, we measured PPR of cortical EPSCs in BA PV-INs. This revealed no change in glutamate release in trained animals (Figure 4G–I), consistent with a lack of modulation of mEPSC frequency by learning in BA PV-INs (Figure 3I).

Presynaptic Origins of Subcortical and Cortical Afferent Plasticity

Although electrical stimulation of the internal and external capsules is presumed to recruit glutamatergic axons from sensory thalamus and cortex, respectively, we sought to characterize this circuitry using region- and cell-selective tools. To determine the presynaptic origins of PV-IN innervation, we conducted unbiased Cre-dependent monosynaptic circuit tracing (Watabe-Uchida et al., 2012; Wickersham et al., 2007). AAVs encoding conditional expression of the TVA receptor and rabies glycoprotein (G) were unilaterally injected into the basolateral amygdala of PV-IRES-Cre mice, restricting subsequent infection of G-deleted rabies virus (RV*d*G) pseudotyped with the envelop protein A (EnvA) to PV-INs and their retrograde monosynaptic contacts (Figure 5A). In addition to other subcortical and cortical regions (Figure S5), amygdala PV-INs received robust innervation from the medial geniculate nucleus (MGN) and the temporal association cortex (TeA; Figure 5B–C). These regions are known to convey auditory input to amygdala and their axon terminals are presumed to be involved in plasticity of internal and external capsule synaptic responses in amygdala excitatory neurons (Ledoux, J.E., 2000).

To investigate functional synaptic connectivity between MGN/TeA and amygdala PV-INs, we targeted these areas with injections of an AAV encoding eYFP-tagged channelrhodopsin 2 (ChR2-eYFP) driven by the CaMKII promoter in PV-IRES-Cre:Ai9 double transgenic mice, in which tdTomato expression is localized to PV-INs. Following these injections, eYFP+ terminals were observed in the basolateral amygdala complex. However, MGN

terminals were largely restricted to LA, whereas TeA terminals could be observed in both LA and BA (Figure 5D–E). Terminal stimulation evoked polysynaptic EPSCs in PV-INs (Fig. 5F), likely the result of strong local excitatory connections to PV-INs. To isolate monosynaptic currents, we blocked NMDA receptors with saturating CPP (10 μM) and AMPA receptors with subsaturating CNQX (1 μM). Resulting optic-evoked EPSCs (oEPSCs) could be completely abolished with saturating CNQX (10 μM; Figure 5F). Consistent with anatomical labeling, blue-light stimulation of MGN terminals resulted in monosynaptic oEPSCs in the vast majority of LA PV-INs (36/41), but no responses were detected in BA PV-INs (0/10). In contrast, oEPSCs were observed in both LA (28/35) and BA (27/30) PV-INs during TeA terminal stimulation (Figure 5G). Onset latencies of oEPSCs were consistent with monosynaptic transmission (Figure 5H).

We next measured PPR of oEPSCs to determine whether MGN and TeA afferent plasticity could account for learning-dependent changes in glutamate release (Figure 4). Surprisingly, this revealed no effect of fear conditioning on PPR at MGN synapses onto LA PV-INs (Figure 5I–J). However, consistent with the results of electrical stimulation (Figure 4D–I), PPR of TeA oEPSCs was increased in paired animals relative to both naïve and unpaired controls in LA (repeated-measures ANOVA, main effect of group, $F_{(2,72)} = 12.03$, $p = 0.0002$), but not BA PV-INs (Figure 5K–N). These data confirm the nucleus-specificity of PV-IN afferent plasticity in the auditory cortical pathway but suggest that plasticity of internal capsule responses is not attributable to auditory thalamic inputs.

Nucleus- and Synapse-Specific Reduction of GABA release from PV-INs

Previous studies suggest that changes in inhibitory transmission may occur after fear conditioning, but this work relied mainly on analysis of GABA receptors from amygdala lysates (Chhatwal et al., 2005; Heldt and Ressler, 2007; Lin et al., 2011). It therefore remains unclear whether fear encoding alters GABA transmission within specific microcircuits. To enable stimulation of synapses formed by PV-INs, we injected Cre-inducible AAV vectors encoding ChR2-eYFP into PV-IRES-Cre mice, resulting in somal and axonal eYFP expression in PV-INs (Figure 6A–B) and blue-light driven action potential generation (Figure 6C). Consistent with selective recombination in PV-INs (Figure 1A, Figure S1), we verified that optic stimulation in these mice did not result in non-GABAergic transmission (Figure 6D–F). Nevertheless, subsequent experiments were conducted in the presence of glutamate receptor antagonists. We used paired-pulse optic stimulation ($\lambda = 470$ nm) to determine whether fear conditioning leads to changes in GABA release from PV-INs onto neighboring principal neurons. Repeated-measured ANOVA revealed that PPR differed between conditions in the LA (repeated-measures ANOVA, main effect of group, $F_{(2,68)} = 26.13$, $p < 0.001$) but not in the BA. In LA, PPR was increased in paired, but not unpaired, animals relative to naïve controls. This decrease in GABA release was at least partly specific to PV-IN inputs because IPSCs evoked by local field stimulation were not modulated by training (Figure S6A–C).

To determine whether PV-IN-specific plasticity corresponds to an overall reduction of inhibition onto LA principal neurons, we collected spontaneous IPSCs (sIPSCs) from these cells after fear conditioning. Consistent with a previous report (Lin et al., 2011), both sIPSC

frequency (one-way ANOVA, F (2,51) = 11.17, $p = 0.0001$) and amplitude (one-way ANOVA, F(2,51) = 6.80, $p = 0.003$) was decreased in LA of animals that received paired training (Figure S6D–G). However, no changes in sIPSC properties were observed in BA principal neurons (Figure S6H–K). While our data suggest that decreased GABA release from PV-INs may contribute to reduced sIPSC frequency in LA, it is important to consider that these events reflect the cumulative action of GABA transmission not only from PV-INs but also from other inhibitory cell types.

Given the dense innervation of PV-INs by other PV-INs in the BA (Muller et al., 2005; Woodruff and Sah, 2007), we next questioned whether the observed changes in GABA release are specific to glutamatergic targets, in particular because fear conditioning altered mIPSC frequency in BA PV-INs (Figure 3L). To facilitate fluorescence-based targeting of PV-INs without activating ChR2, we injected Cre-dependent AAV-ChR2 into the amygdala of PV-IRES-Cre:Ai9 transgenic mice (Figure 6K). This strategy allowed us to use non-overlapping LED spectra for PV-IN visualization and ChR2 excitation (Figure 6L). PPR analysis of PV-IN → PV-IN oIPSCs revealed no learning-induced differences in GABA release in LA or BA (Figure 6M–P), indicating that, in addition to being nucleus-specific, learning-dependent changes in PVIN inhibition exhibit target selectivity.

A previous report found that fear conditioning induces alterations in GABA receptor expression in the lateral amygdala that are reversible by extinction (Lin et al., 2011). Therefore, we postulated that GABA release properties might exhibit similar bidirectional regulation. However, increased PPR of PV-IN IPSCs was not reversed by extinction training (Figure S7).

Intrinsic Excitability of Basolateral Amygdala PV-INs is Unaltered by Fear Memory Encoding

While synapse-selective changes can alter the relationship of PV-INs to specific pre- and postsynaptic targets, firing rate plasticity could render PV-INs more or less excitable and thus impact their general integration. To evaluate this possibility, we examined action potential discharge in PV-INs in response to somatic current injections after fear conditioning. No experience-dependent differences in firing frequency were observed in LA or BA (Figure 7A–F). In naïve animals, however, PV-INs in BA were more excitable than those in LA (Figure 7G), exhibiting reduced rheobase current (independent samples t-test, $t_{(23)} = 2.19$, $p = 0.04$) and increased firing frequency (repeated-measure ANOVA, main effect of nucleus, $F_{(1, 207)} = 17.81$, $p = 0.0003$). This nucleus-specific difference is likely attributable to increased cell size, as inferred from a difference in online capacitance measurements from PV-INs (LA 125.59 ± 15.40 pF; BA 77.36 ± 7.60 pF; independent-samples t-test, $t_{(11)} = 2.98$, $p = 0.01$). No other differences in passive membrane properties were observed. Likewise, no differences were observed in individual spike characteristics (including threshold, amplitude, duration, or after hyperpolization; Figure 7H–K).

Discussion

With the aid of cell-selective reporters and optogenetic tools, we achieved several novel insights into amygdala PV-IN function. First, the amygdala is populated by two distinct

networks of PV-INs defined by their nucleus location, dendritic complexity, and potency of afferent excitation. Second, these striking differences correlate with the preferential engagement of LA, but not BA, PV-INs in afferent-evoked feedforward inhibition. Third, fear memory encoding results in selective functional downregulation of LA PV-IN microcircuitry through plasticity of both afferent input as well as GABA release. Importantly, input plasticity could be localized in part to projections from TeA, an auditory cortical region that displays increased CS-related activity after fear acquisition (Quirk et al., 1997). Together, our studies point to multimodal plasticity of discrete PV-IN microcircuits as potentially integral to aversive memory encoding. Decreased PV-IN activity would be expected to enhance recruitment of amygdala excitatory projection neurons and corresponding fear-related behaviors by sensory stimulation.

Several recent studies indicate that feedforward engagement of PV-INs in the cortex is pathway-specific (Delevich et al., 2015; Lee et al., 2014; Li et al., 2014; Rock and Apicella, 2015; Yang et al., 2013). Here we show that such differential recruitment also occurs among amygdala PV-IN subpopulations within the same afferent pathway and is correlated with PV-IN morphological and physiological specialization. A likely explanation for increased excitatory drive in LA PV-INs is that they possess more dendritic compartments and a corresponding greater number of afferent synapses. On the other hand, the lack of feedforward inhibition from BA PV-INs is consistent with anatomical data suggesting that amygdala PV-INs are minimally targeted by cortical afferents (Smith et al., 2000), even though our results establish that the majority of BA PV-INs can be driven by cortical stimulation. However, this and other studies have largely focused on BA PV-INs, neglecting a comparatively sparse population of LA PV-INs that apparently compensate for their smaller numbers with greater excitatory drive. Indeed, while our viral injections led to eArch3.0 expression in an average of only 2–4 LA PV-INs per brain slice (Figure S2A), light-evoked suppression of these cells was surprisingly effective at reducing feedforward inhibition. Potent recruitment of PV-INs by subcortical and cortical pathways may in part explain the relative silence of LA, compared to other amygdala nuclei, when sampled by *in vivo* electrodes (Gaudreau and Pare, 1996). Such properties also make PV-INs a potentially powerful substrate for experience-dependent gain modulation of amygdala input.

Past research has established an important role for excitatory synaptic strengthening within amygdala afferent pathways during the encoding of cued fear associations (Janak and Tye, 2015; Johansen et al., 2011; Nabavi et al., 2014). Although far less advanced, research into amygdala inhibitory transmission has suggested that memory encoding also alters GABAergic neuronal substrates (Chhatwal et al., 2005; Heldt and Ressler, 2007; Lin et al., 2011). Interestingly, whereas excitation and inhibition are co-upregulated in *ex vivo* preparations during the expression of long-term potentiation (Lamsa et al., 2005), our work indicates that glutamatergic (Arruda-Carvalho and Clem, 2014; Clem and Huganir, 2010, 2013) and GABAergic function (present study) are modified in opposite directions following emotional learning. In contrast to excitatory neuronal plasticity, which involves pre- and postsynaptic alterations as well as changes in membrane excitability (Johansen et al., 2011; Sigurdsson et al., 2007), PV-IN plasticity was localized to presynaptic compartments. Similar to our findings, a recent study reported that intercalated GABAergic projection neurons that surround the basolateral amygdala display decreased glutamatergic responses

following fear conditioning (Asede et al., 2015). To our knowledge, however, ours is the first study to describe plasticity of GABA release following associative learning. Since target-selective structural plasticity has been observed in PV-INs after extinction training (Trouche et al., 2013), it seems that dynamic regulation of PV-IN terminals could be a fundamental mechanism of emotional learning. However, we did not observe reversal of decreased GABA release onto principal neurons after extinction learning (Figure S7), indicating different modes of experience-dependent plasticity may govern the role of amygdala PV-INs in fear conditioning and extinction.

The mechanisms mediating decreased transmission from PV-INs after fear learning are currently unknown. Upregulation of both parvalbumin and glutamic acid decarboxylase 67 (GAD67, a GABA synthetic enzyme) in PV-INs has been proposed to be a signature of memory encoding across multiple paradigms and brain regions, including in the hippocampus after contextual fear conditioning (Donato et al., 2013). These changes would be predicted to decrease PPR of oIPSCs due to increased GABA stores as well as enhanced calcium buffering capacity of PV-INs (Caillard et al., 2000). However, our data show that these findings may not extrapolate to the amygdala, where fear conditioning leads to a decrease in PPR of PV-IN-mediated oIPSCs.

On the other hand, recently described effects of neuromodulators on PV-IN release properties suggest their potential involvement in fear-related inhibitory plasticity. Dopaminergic terminals form dense perisomatic synapses onto amygdala PV-INs (Brinley-Reed and McDonald, 1999; Pinard et al., 2008), and *ex vivo* dopamine application acts through D2 receptors to reduce GABA release from PV-INs (Chu et al. 2012). Similar to fear conditioning (Figure 6), dopamine effects are manifested at PV-IN synapses onto principal cells but not interneurons. In addition, D2 receptor activation reduces the frequency of sIPSCs as well as the magnitude of principal neuron feedforward inhibition in LA (Bissiere et al., 2003). Thus, dopamine release may be a key mechanism leading to PV-IN plasticity and corresponding amygdala disinhibition.

An intriguing outcome of our optogenetic interrogations was that MGN terminals did not exhibit changes in glutamate release onto PV-INs following fear conditioning (Figure 5), as predicted based on electrical stimulation of the internal capsule (Figure 4A–C), in which MGN axons could be detected based on eYFP fluorescence. It seems unlikely that thalamic expression of ChR2 prevented or occluded plasticity, since changes in PPR were readily observed at TeA synapses. Therefore, we suggest that internal capsule stimulation recruits other subcortical projections whose modification may be important for auditory fear conditioning. Future experiments should examine whether these projections also account for previously described plasticity of internal capsule EPSCs in principal neurons (Clem and Huganir, 2010, 2013; McKernan et al., 1997; Namburi et al., 2015; Rumpel et al., 2005; Tye et al., 2008; Zhou et al., 2009), a finding that would upend the conventional wisdom that excitatory synaptic strengthening is attributable to the auditory thalamic pathway. It is worth noting, however, that even though MGN synapses were unaffected by training, feedforward inhibition from this pathway could nevertheless be modulated by decreased output of PV-INs (Figure 6).

Another important unanswered question is which neuronal population(s) are responsible for enhanced inhibition onto PV-INs in BA after fear learning (Figure 3L). While PV-INs are densely interconnected in this region (Muller et al., 2005; Woodruff and Sah, 2007), GABA release at PV-IN → PV-IN synapses was not modulated by fear encoding (Figure 6), indicating that another GABAergic population is responsible for this effect. Although recordings from sensory cortex point to somatostatin-containing interneurons as major regulators of PV-INs (Pfeffer et al., 2013; Xu et al., 2013), only a very small percentage of somatostatin-positive terminals form synapses with PV-INs in amygdala (Muller et al., 2007). However, the GABAergic cells that mediate inhibitory plasticity are not necessarily intrinsic to the amygdala and may be connected to PV-INs through long-range projections, such as those arising from the basal forebrain that densely and selectively terminate onto PV-INs in the BA but not LA (McDonald et al., 2011). Future studies will be required examine the contributions of intrinsic and extrinsic GABAergic populations to experience-dependent plasticity in amygdala PV-IN microcircuits.

Regarding the outcomes of real-life traumatic experiences, the various forms of PV-IN-specific plasticity that we describe could contribute to amygdala hyperexcitability as well as generalization of conditioned fear to nonspecific stimuli, which in certain cases may serve an evolutionarily adaptive purpose. However, such plasticity may also be a precipitating factor for escalating fear and anxiety in PTSD. Indeed, preclinical animal models suggest that PV-IN dysfunction may be involved in pathological, extinction-resistant fear (Bissonette et al., 2014; Brown et al., 2015; Lucas et al., 2014). Therefore, experiments should examine whether chronic stress or trauma is associated with altered inhibitory plasticity and whether these effects may underlie progression to emotional dysfunction. Our results provide an initial framework for elucidating these roles by clarifying the basic function of PV-IN microcircuits and their modification by aversive conditioning.

Experimental Procedures

Further details can be found in the Supplemental Experimental Procedures.

Animals

All experiments were approved in advance by the Institutional Care and Use Committee of the Icahn School of Medicine at Mount Sinai. Experiments were conducted on male mice 28–40 days of age from the following lines: C56Bl/6J (RRID:IMSR_JAX:000664), PV-IRES-Cre (RRID:IMSR_JAX:008069), R26-STOP-eYFP (RRID:IMSR_JAX:006148), and Rosa-CAG-LSL-tdTomato-WPRE (Ai9; RRID:IMSR_JAX:007909).

Viral targeting for electrophysiology

Viral constructs were purchased from the University of Pennsylvania Vector Core and included AAV1-EF1a-DIO-hChR2(H134R)-eYFP-WPRE (Addgene #20298), AAV1-CBA-Flex-Arch-GFP (Addgene #22222), and AAV1-CamKIIa-hChR2(H134R)-eYFP-WPRE (Addgene #26969P). Viral constructs (0.3–1 μL) were bilaterally injected into the basolateral amygdala (AP −1.4, ML ±3.3, DV −5.0), temporal association cortex (AP −4.0, ML ±4.0, DV −3.5), and medial geniculate nucleus (AP −3.2, ML ±1.8, DV −3.5).

Viral targeting for monosynaptic circuit tracing

Viral constructs were purchased from the University of North Carolina Vector Core (AAV8-EF1a-FLEX-TVA-mCherry, Addgene #38044; AAV8-CA-FLEX-RG, Addgene #38043; Watabe-Uchida et al., 2012) and the Salk Institute Gene Transfer, Targeting, and Therapeutics Core (EnvA G-deleted Rabies-eGFP, Addgene #32635; Wickersham et al., 2010). Unilateral basolateral amygdala injections of AAV8-EF1a-FLEX-TVA-mCherry and AAV8-CA-FLEX-RG (1:1 ratio) were conducted three weeks prior to EnvA G-deleted Rabies-eGFP, and animals were sacrificed by transcardial perfusion one week later.

Immunofluorescence staining

Immunofluoresence was conducted as previously described (Lucas et al., 2014).

Fear conditioning

Cued auditory fear conditioning was conducted in sound attenuating chambers with automated stimulus delivery software (MedAssociates, St. Albans, VT, USA) as previously described (Clem and Huganir, 2010, 2013).

Slice electrophysiology

Acute coronal slices of the basolateral amygdala were prepared as previously described (Clem and Huganir, 2010, 2013). Cells were visualized on an upright DIC microscope equipped with objective-coupled LEDs (460 nm and broad spectrum (white); Prizmatix, Givat-Shmuel, Israel) for the identification of fluorescence- cells as well as optogenetic cellular manipulations. Data were low-pass filtered at 3 kHz (evoked) and 10 kHz (spontaneous, miniature) and acquired at 10 kHz using Multiclamp 700B and pClamp 10 (Molecular Devices, Sunnyvale, CA, USA). Evoked data were analyzed in Clampfit 10 (Molecular Devices); spontaneous and miniature currents were analyzed with MiniAnalysis (Synaptosoft, Fort Lee, NJ, USA). All data analyses were conducted blind to the experimental group.

Morphological Analysis

Live brain sections were prepared as for slice electrophysiology. PV-INs were identified by tdTomato expression, patched, and filled with 0.5% biocytin. Tissue preparation and morphological analyses were conducted as previously described (Dougherty et al., 2014).

Statistics

Two-tail paired t-tests (one group), two-tail independent samples t-tests (two groups), one-way ANOVA (≥ 3 groups), two-way ANOVA (≥ 2 groups with ≥ 2 variables), or two-way repeated-measured ANOVA (≥ 2 groups with repeating variable) were implemented to determine statistical significance. All posthoc tests were chosen to maintain family wise error rate at 0.05. Data are presented as mean ± standard error of the mean (SEM) with n as the number of cells followed by the number of animals in parentheses.

Supplementary Material

Refer to Web version on PubMed Central for supplementary material.

Acknowledgments

This work was funded by NIH grants MH105414 (R.L.C), EY026053 (H.M.), and MH096678 (E.K.L), a NARSAD Young Investigator Award (R.L.C.), and seed funds from the Friedman Brain Institute at the Icahn School of Medicine at Mount Sinai. We would like to thank Timothy Rumbell for instruction on spike analysis, Dara Dickstein and Katina Calakos for assistance with morphological analysis, Elisa Nabel for guidance on Cre-dependent monosynaptic input mapping, Stephen Salton for sharing his equipment, and Karl Deisseroth, Ed Boyden, Ed Callaway, and Naoshige Uchida for their generous contribution of viral vectors.

References

Arruda-Carvalho M, Clem RL. Pathway-selective adjustment of prefrontal-amygdala transmission during fear encoding. J. Neurosci. 2014; 34:15601–15609. [PubMed: 25411488]

Asede D, Bosch D, Luthi A, Ferraguti F, Ehrlich I. Sensory inputs to intercalated cells provide fear-learning modulated inhibition to the basolateral amygdala. Neuron. 2015; 86:541–554. [PubMed: 25843406]

Bauer EP, LeDoux JE. Heterosynaptic long-term potentiation of inhibitory interneurons in the lateral amygdala. J. Neurosci. 2004; 24:9507–9512. [PubMed: 15509737]

Bienvenu TC, Busti D, Magill PJ, Ferraguti F, Capogna M. Cell-type-specific recruitment of amygdala interneurons to hippocampal theta rhythm and noxious stimuli in vivo. Neuron. 2012; 74:1059–1074. [PubMed: 22726836]

Bissiere S, Humeau Y, Luthi A. Dopamine gates LTP induction in lateral amygdala by suppressing feedforward inhibition. Nat. Neurosci. 2003; 6:587–592. [PubMed: 12740581]

Bissonette GB, Bae MH, Suresh T, Jaffe DE, Powell EM. Prefrontal cognitive deficits in mice with altered cerebral cortical GABAergic interneurons. Behav. Brain Res. 2014; 259:143–151. [PubMed: 24211452]

Bremner JD, Innis RB, Southwick SM, Staib L, Zoghbi S, Charney DS. Decreased benzodiazepine receptor binding in prefrontal cortex in combat-related posttraumatic stress disorder. Am. J. Psychiatry. 2000; 157:1120–1126. [PubMed: 10873921]

Brinley-Reed M, McDonald AJ. Evidence that dopaminergic axons provide a dense innervation of specific neuronal subpopulations in the rat basolateral amygdala. Brain Res. 1999; 850:127–135. [PubMed: 10629756]

Brown JA, Ramikie TS, Schmidt MJ, Baldi R, Garbett K, Everheart MG, Warren LE, Gellert L, Horvath S, Patel S, et al. Inhibition of parvalbumin-expressing interneurons results in complex behavioral changes. Mol. psychiatry. 2015

Caillard O, Moreno H, Schwaller B, Llano I, Celio MR, Marty A. Role of the calcium-binding protein parvalbumin in short-term synaptic plasticity. Proc. Natl. Acad. Sci. USA. 2000; 97:13372–13377. [PubMed: 11069288]

Chhatwal JP, Myers KM, Ressler KJ, Davis M. Regulation of gephyrin and GABAA receptor binding within the amygdala after fear acquisition and extinction. J. Neurosci. 2005; 25:502–506. [PubMed: 15647495]

Chow BY, Han X, Dobry AS, Qian X, Chuong AS, Li M, Henninger MA, Belfort GM, Lin Y, Monahan PE, et al. High-performance genetically targetable optical neural silencing by light-driven proton pumps. Nature. 2010; 463:98–102. [PubMed: 20054397]

Chu HY, Ito W, Li J, Morozov A. Target-specific suppression of GABA release from parvalbumin interneurons in the basolateral amygdala by dopamine. The J. Neurosci. 2012; 32:14815–14820. [PubMed: 23077066]

Clem RL, Huganir RL. Calcium-permeable AMPA receptor dynamics mediate fear memory erasure. Science. 2010; 330:1108–1112. [PubMed: 21030604]

Clem RL, Huganir RL. Norepinephrine enhances a discrete form of long-term depression during fear memory storage. J. Neurosci. 2013; 33:11825–11832. [PubMed: 23864672]

Courtin J, Chaudun F, Rozeske RR, Karalis N, Gonzalez-Campo C, Wurtz H, Abdi A, Baufreton J, Bienvenu TC, Herry C. Prefrontal parvalbumin interneurons shape neuronal activity to drive fear expression. Nature. 2014; 505:92–96. [PubMed: 24256726]

Delevich K, Tucciarone J, Huang ZJ, Li B. The mediodorsal thalamus drives feedforward inhibition in the anterior cingulate cortex via parvalbumin interneurons. J. Neurosci. 2015; 35:5743–5753. [PubMed: 25855185]

Donato F, Rompani SB, Caroni P. Parvalbumin-expressing basket-cell network plasticity induced by experience regulates adult learning. Nature. 2013; 504:272–276. [PubMed: 24336286]

Dorrn AL, Yuan K, Barker AJ, Schreiner CE, Froemke RC. Developmental sensory experience balances cortical excitation and inhibition. Nature. 2010; 465:932–936. [PubMed: 20559387]

Dougherty SE, Bartley AF, Lucas EK, Hablitz JJ, Dobrunz LE, Cowell RM. Mice lacking the transcriptional coactivator PGC-1α exhibit alterations in inhibitory synaptic transmission in the motor cortex. Neuroscience. 2014; 271:137–148. [PubMed: 24769433]

Feusner J, Ritchie T, Lawford B, Young RM, Kann B, Noble EP. GABA(A) receptor beta 3 subunit gene and psychiatric morbidity in a post-traumatic stress disorder population. Psychiatry Res. 2001; 104:109–117. [PubMed: 11711165]

Gaudreau H, Pare D. Projection neurons of the lateral amygdaloid nucleus are virtually silent throughout the sleep--waking cycle. J. Neurophysiol. 1996; 75:1301–1305. [PubMed: 8867138]

Geuze E, van Berckel BN, Lammertsma AA, Boellaard R, de Kloet CS, Vermetten E, Westenberg HG. Reduced GABAA benzodiazepine receptor binding in veterans with post-traumatic stress disorder. Mol. Psychiatry. 2008; 13:74–83. 73. [PubMed: 17667960]

Hangya B, Pi HJ, Kvitsiani D, Ranade SP, Kepecs A. From circuit motifs to computations: mapping the behavioral repertoire of cortical interneurons. Curr. Opin. Neurobio. 2014; 26:117–124.

Heldt SA, Ressler KJ. Training-induced changes in the expression of GABAA-associated genes in the amygdala after the acquisition and extinction of Pavlovian fear. Eur. J. Neurosci. 2007; 26:3631–3644. [PubMed: 18088283]

House DR, Elstrott J, Koh E, Chung J, Feldman DE. Parallel regulation of feedforward inhibition and excitation during whisker map plasticity. Neuron. 2011; 72:819–831. [PubMed: 22153377]

Hu H, Gan J, Jonas P. Interneurons. Fast-spiking, parvalbumin(+) GABAergic interneurons: from cellular design to microcircuit function. Science. 2014; 345:1255263. [PubMed: 25082707]

Janak PH, Tye KM. From circuits to behaviour in the amygdala. Nature. 2015; 517:284–292. [PubMed: 25592533]

Johansen JP, Cain CK, Ostroff LE, LeDoux JE. Molecular mechanisms of fear learning and memory. Cell. 2011; 147:509–524. [PubMed: 22036561]

Katagiri H, Fagiolini M, Hensch TK. Optimization of somatic inhibition at critical period onset in mouse visual cortex. Neuron. 2007; 53:805–812. [PubMed: 17359916]

Lamsa K, Heeroma JH, Kullmann DM. Hebbian LTP in feed-forward inhibitory interneurons and the temporal fidelity of input discrimination. Nat. Neurosci. 2005; 8:916–924. [PubMed: 15937481]

Ledoux JE. Emotion circuits in the brain. Annual Review of Neuroscience. 2000; 23:155–184.

Lee AT, Gee SM, Vogt D, Patel T, Rubenstein JL, Sohal VS. Pyramidal neurons in prefrontal cortex receive subtype-specific forms of excitation and inhibition. Neuron. 2014; 81:61–68. [PubMed: 24361076]

Letzkus JJ, Wolff SB, Meyer EM, Tovote P, Courtin J, Herry C, Luthi A. A disinhibitory microcircuit for associative fear learning in the auditory cortex. Nature. 2011; 480:331–335. [PubMed: 22158104]

Li LY, Ji XY, Liang F, Li YT, Xiao Z, Tao HW, Zhang LI. A feedforward inhibitory circuit mediates lateral refinement of sensory representation in upper layer 2/3 of mouse primary auditory cortex. J. Neurosci. 2014; 34:13670–13683. [PubMed: 25297094]

Lin HC, Tseng YC, Mao SC, Chen PS, Gean PW. GABAA receptor endocytosis in the basolateral amygdala is critical to the reinstatement of fear memory measured by fear-potentiated startle. J. Neurosci. 2011; 31:8851–8861. [PubMed: 21677169]

Lucas EK, Jegarl A, Clem RL. Mice lacking TrkB in parvalbumin-positive cells exhibit sexually dimorphic behavioral phenotypes. Behav. Brain Res. 2014; 274:219–225. [PubMed: 25127683]

Mahan AL, Ressler KJ. Fear conditioning, synaptic plasticity and the amygdala: implications for posttraumatic stress disorder. Trends Neurosci. 2012; 35:24–35. [PubMed: 21798604]

Mahanty NK, Sah P. Calcium-permeable AMPA receptors mediate long-term potentiation in interneurons in the amygdala. Nature. 1998; 394:683–687. [PubMed: 9716132]

McDonald AJ, Mascagni F. Colocalization of calcium-binding proteins and GABA in neurons of the rat basolateral amygdala. Neuroscience. 2001; 105:681–693. [PubMed: 11516833]

McDonald AJ, Muller JF, Mascagni F. Postsynaptic targets of GABAergic basal forebrain projections to the basolateral amygdala. Neuroscience. 2011; 183:144–159. [PubMed: 21435381]

McKernan MG, Shinnick-Gallagher P. Fear conditioning induces a lasting potentiation of synaptic currents in vitro. Nature. 1997; 390:607–611. [PubMed: 9403689]

Meyerhoff DJ, Mon A, Metzler T, Neylan TC. Cortical gamma-aminobutyric acid and glutamate in posttraumatic stress disorder and their relationships to self-reported sleep quality. Sleep. 2014; 37:893–900. [PubMed: 24790267]

Muller JF, Mascagni F, McDonald AJ. Coupled networks of parvalbumin-immunoreactive interneurons in the rat basolateral amygdala. J. Neurosci. 2005; 25:7366–7376. [PubMed: 16093387]

Muller JF, Mascagni F, McDonald AJ. Pyramidal cells of the rat basolateral amygdala: synaptology and innervation by parvalbumin-immunoreactive interneurons. J. Comp. Neurol. 2006; 494:635–650. [PubMed: 16374802]

Muller JF, Mascagni F, McDonald AJ. Postsynaptic targets of somatostatin-containing interneurons in the rat basolateral amygdala. J. Comp. Neurol. 2007; 500:513–529. [PubMed: 17120289]

Namburi P, Beyeler A, Yorozu S, Calhoon GG, Halbert SA, Wichmann R, Holden SS, Mertens KL, Anahtar M, Felix-Ortiz AC, et al. A circuit mechanism for differentiating positive and negative associations. Nature. 2015; 520:675–678. [PubMed: 25925480]

Nabavi S, Fox R, Proulx CD, Lin JY, Tsien RY, Manilow R. Engineering a memory with LTD and LTP. Nature. 2014; 511:348–352. [PubMed: 24896183]

Pennington DL, Abe C, Batki SL, Meyerhoff DJ. A preliminary examination of cortical neurotransmitter levels associated with heavy drinking in posttraumatic stress disorder. Psychiatry Res. 2014; 224:281–287. [PubMed: 25444536]

Pfeffer CK, Xue M, He M, Huang ZJ, Scanziani M. Inhibition of inhibition in visual cortex: the logic of connections between molecularly distinct interneurons. Nat. Neurosci. 2013; 16:1068–1076. [PubMed: 23817549]

Pinard CR, Muller JF, Mascagni F, McDonald AJ. Dopaminergic innervation of interneurons in the rat basolateral amygdala. Neuroscience. 2008; 157:850–863. [PubMed: 18948174]

Polepalli JS, Sullivan RK, Yanagawa Y, Sah P. A specific class of interneuron mediates inhibitory plasticity in the lateral amygdala. J. Neurosci. 2010; 30:14619–14629. [PubMed: 21048119]

Quirk GJ, Armony JL, LeDoux JE. Fear conditioning enhances different temporal components of tone-evoked spike trains in auditory cortex and lateral amygdala. Neuron. 1997; 19:613–624. [PubMed: 9331352]

Rock C, Apicella AJ. Callosal projections drive neuronal-specific responses in the mouse auditory cortex. J. Neurosci. 2015; 35:6703–6713. [PubMed: 25926449]

Rossi S, De Capua A, Tavanti M, Calossi S, Polizzotto NR, Mantovani A, Falzarano V, Bossini L, Passero S, Bartalini S, et al. Dysfunctions of cortical excitability in drug-naive posttraumatic stress disorder patients. Bio. Psychiatry. 2009; 66:54–61. [PubMed: 19368897]

Rosso IM, Weiner MR, Crowley DJ, Silveri MM, Rauch SL, Jensen JE. Insula and anterior cingulate GABA levels in posttraumatic stress disorder: preliminary findings using magnetic resonance spectroscopy. Depress Anxiety. 2014; 31:115–123. [PubMed: 23861191]

Rumpel S, LeDoux J, Zador A, Malinow R. Postsynaptic receptor trafficking underlying a form of associative learning. Science. 2005; 308:83–88. [PubMed: 15746389]

Sah P, Faber ES, Lopez De Armentia M, Power J. The amygdaloid complex: anatomy and physiology. Physiol. Rev. 2003; 83:803–834. [PubMed: 12843409]

Shin RM, Tsvetkov E, Bolshakov VY. Spatiotemporal asymmetry of associative synaptic plasticity in fear conditioning pathways. Neuron. 2006; 52:883–896. [PubMed: 17145508]

Sigurdsson T, Doyere V, Cain CK, LeDoux JE. Long-term potentiation in the amygdala: a cellular mechanism of fear learning and memory. Neuropharmacology. 2007; 52:215–227. [PubMed: 16919687]

Smith Y, Pare JF, Pare D. Differential innervation of parvalbumin-immunoreactive interneurons of the basolateral amygdaloid complex by cortical and intrinsic inputs. J. Comp. Neurol. 2000; 416:496–508. [PubMed: 10660880]

Szinyei C, Heinbockel T, Montagne J, Pape HC. Putative cortical and thalamic inputs elicit convergent excitation in a population of GABAergic interneurons of the lateral amygdala. J. Neurosci. 2000; 20:8909–8915. [PubMed: 11102501]

Trouche S, Sasaki JM, Tu T, Reijmers LG. Fear extinction causes target-specific remodeling of perisomatic inhibitory synapses. Neuron. 2013; 80:1054–1065. [PubMed: 24183705]

Turner BH, Herkenham M. Thalamoamygdaloid projections in the rat: a test of the amygdala's role in sensory processing. J. Comp. Neurol. 1991; 313:295–325. [PubMed: 1765584]

Tye KM, Stuber GD, de Ridder B, Bonci A, Janak PH. Rapid strengthening of thalamo-amygdala synapses mediates cue-reward learning. Nature. 2008; 453:1253–1257. [PubMed: 18469802]

Vaiva G, Boss V, Ducrocq F, Fontaine M, Devos P, Brunet A, Laffargue P, Goudemand M, Thomas P. Relationship between posttrauma GABA plasma levels and PTSD at 1-year follow-up. Am. J. Psychiatry. 2006; 163:1446–1448. [PubMed: 16877663]

Vaiva G, Thomas P, Ducrocq F, Fontaine M, Boss V, Devos P, Rascle C, Cottencin O, Brunet A, Laffargue P, et al. Low posttrauma GABA plasma levels as a predictive factor in the development of acute posttraumatic stress disorder. Bio. Psychiatry. 2004; 55:250–254. [PubMed: 14744465]

Vogels TP, Sprekeler H, Zenke F, Clopath C, Gerstner W. Inhibitory plasticity balances excitation and inhibition in sensory pathways and memory networks. Science. 2011; 334:1569–1573. [PubMed: 22075724]

Watabe-Uchida M, Zhu L, Ogawa SK, Vamanrao A, Uchida N. Whole-brain mapping of direct inputs to midbrain dopamine neurons. Neuron. 2012; 74:858–873. [PubMed: 22681690]

Wickersham IR, Lyon DC, Barnard RJ, Mori T, Finke S, Conzelmann KK, Young JA, Callaway EM. Monosynaptic restriction of transsynaptic tracing from single, genetically targeted neurons. Neuron. 2007; 53:639–647. [PubMed: 17329205]

Wolff SB, Grundemann J, Tovote P, Krabbe S, Jacobson GA, Muller C, Herry C, Ehrlich I, Friedrich RW, Letzkus JJ, et al. Amygdala interneuron subtypes control fear learning through disinhibition. Nature. 2014; 509:453–458. [PubMed: 24814341]

Woodruff AR, Sah P. Networks of parvalbumin-positive interneurons in the basolateral amygdala. J. Neurosci. 2007; 27:553–563. [PubMed: 17234587]

Xu H, Jeong HY, Tremblay R, Rudy B. Neocortical somatostatin-expressing GABAergic interneurons disinhibit the thalamorecipient layer 4. Neuron. 2013; 77:155–167. [PubMed: 23312523]

Yang W, Carrasquillo Y, Hooks BM, Nerbonne JM, Burkhalter A. Distinct balance of excitation and inhibition in an interareal feedforward and feedback circuit of mouse visual cortex. J. Neurosci. 2013; 33:17373–17384. [PubMed: 24174670]

Zhou Y, Won J, Karlsson MG, Zhou M, Rogerson T, Balaji J, Neve R, Poirazi P, Silva AJ. CREB regulates excitability and the allocation of memory to subsets of neurons in the amygdala. Nat Neurosci. 2009; 12:1438–1443. [PubMed: 19783993]

Highlights

- Lateral (LA) but not basal amygdala (BA) PV-INs receive potent afferent excitation.
- PV-INs in LA but not BA mediate feedforward inhibition onto principal neurons.
- Fear conditioning modulates synaptic input to PV-INs in a nucleus-specific manner.
- PV-INs reduce GABA release onto LA principal neurons after fear conditioning.

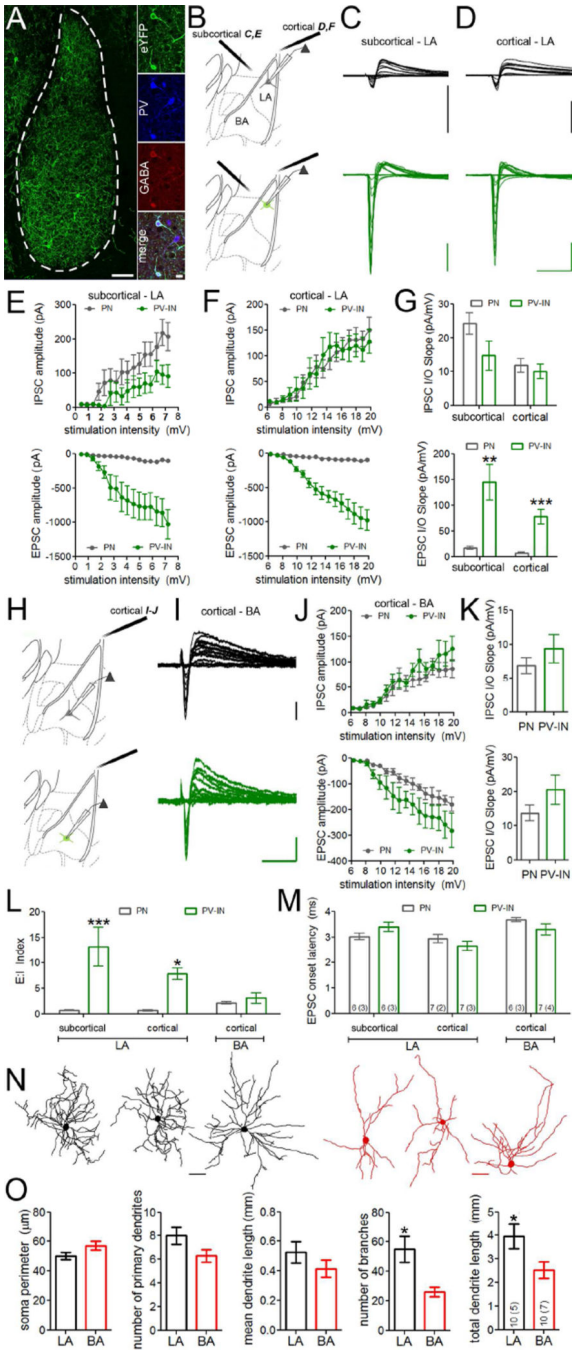

Figure 1. Lateral amygdala parvalbumin-interneurons receive uniquely potent excitatory drive

A. To identify PV-INs for electrophysiological targeting, we crossed PV-IRES-Cre mice to R26-stop-eYFP reporter mice to express eYFP specifically in PV-INs. Double immunofluorescence staining with antibodies against PV (blue) and GAD67 (red) revealed that Cre-dependent eYFP (green) expression selectively labels PV-positive GABAergic neurons in the basolateral complex. Scales = left, 100 µm; right, 20 µm. **B–D**. Lateral amygdala PV-INs and neighboring principal neurons (PNs) respond to subcortical (**C**) and cortical (**D**) afferent stimulation with distinct biphasic synaptic responses, corresponding to

monosynaptic EPSCs followed by disynaptic IPSCs. Scales = 500 pA × 40 ms. **E–F**. Input/output (I/O) relation of lateral amygdala EPSCs and IPSCs during increasing stimulus intensity. **G**. Slope of I/O relation for IPSC (top) and EPSC (bottom) components represented in E and F. **H–J**. Basal amygdala PV-INs and neighboring PNs exhibit similar biphasic EPSC-IPSC responses during cortical afferent stimulation. **I–J**. I/O relation of basal amygdala EPSCs and IPSCs. Scales = 50 pA × 40 ms. **K**. Slope of I/O relation for IPSC (top) and EPSC (bottom) components represented in J. **L**. Excitatory:inhibitory (E:I) balance of biphasic responses for lateral and basal amygdala recordings. I/O index = I/O $slope_{EPSC}$/I/O $slope_{IPSC}$. **M**. Similar onset latency for monosynaptic EPSC components across cells and nuclei. **N**. Representative reconstructions of biocytin-filled PV-INs from lateral (black) and basal (red) amygdala. **O**. Quantification of morphological reconstructions. Membrane potential was clamped at −50 mV for all recordings. n/group indicated on bar histogram in M (C–M) and O. G,L,M two-way ANOVA followed by Holm-Bonferroni. K,O independent samples t-tests. * $p < 0.05$, ** $p < 0.005$, *** $p < 0.0005$. Data presented as mean ± SEM.

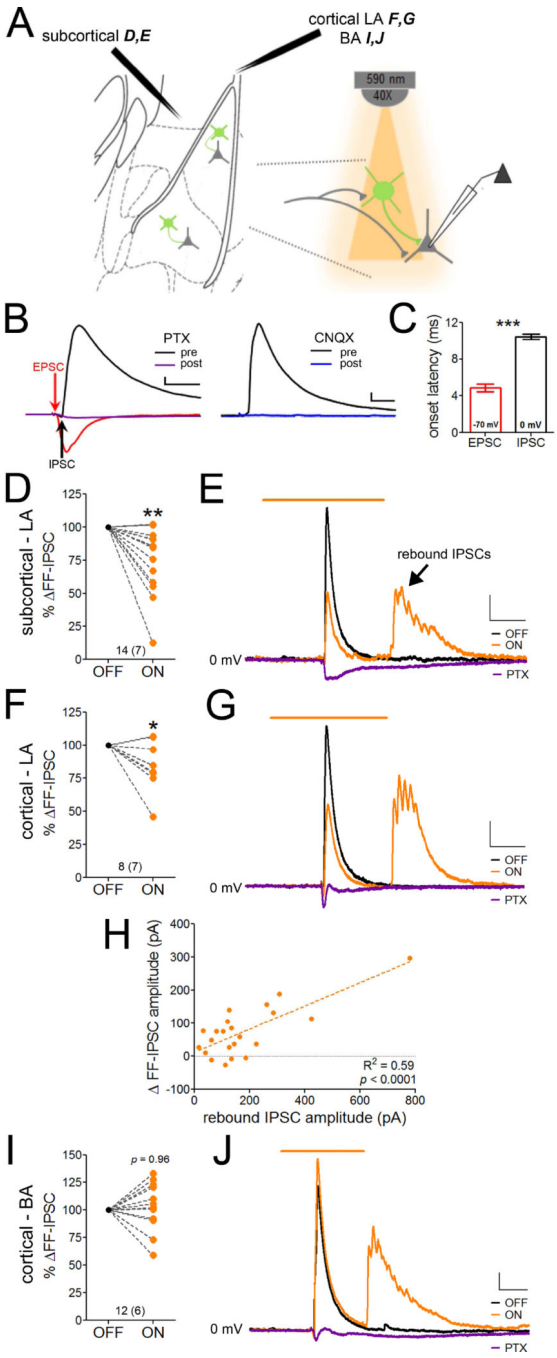

Figure 2. PV-INs mediate feedforward inhibition in the lateral but not the basal amygdala

A. Experimental design in D–J. Subcortical (D,E) and cortical (LA: F,G; BA: I,J) afferents were electrically stimulated to obtain monosynaptic EPSCs and disynaptic IPSCs in LA PNs during voltage clamp at −70 mV and 0 mV, respectively. Electrical stimulation alternated between light-off (n=3) and light-on (n=2) epochs (n=10 sweeps per epoch). **B**. Example traces of monosynaptic excitatory (red trace; −70 mV) and disynaptic inhibitory (black trace; 0 mV) postsynaptic currents evoked from cortical afferents. Disynaptic IPSCs are blocked by the $GABA_A$ receptor antagonist picrotoxin (PTX; purple trace, left) and the

AMPA/kainate receptor antagonist CNQX (blue trace, right). Scales = 70 pA × 20 ms. **C**. Onset latencies of monosynaptic EPSCs and disynaptic IPSCs, shown by arrows in B. **D–G**. Silencing PV-INs attenuated the amplitude of disynaptic IPSCs evoked from subcortical (**D**, representative traces in **E**) and cortical (**F**, representative traces in **G**) afferent stimulation. Evoked IPSCs were blocked by PTX. **H**. Reduction of disynaptic IPSC peak amplitude is correlated with the rebound IPSC amplitude generated at LED offset in LA. **I**. PV-IN silencing did not affect the amplitude of disynaptic IPSCs evoked from cortical afferent stimulation in BA, representative traces in **J**. Scales E,G,J = 50 pA × 100 ms. n/group indicated on graphs. C, independent samples t-test. D,F,I, paired samples t-test. H, linear regression. *$p < 0.05$, **$p < 0.005$, ***$p < 0.0005$. Data in D,F,I are normalized to IPSC amplitude in the absence of LED stimulation. Data presented as mean ± SEM.

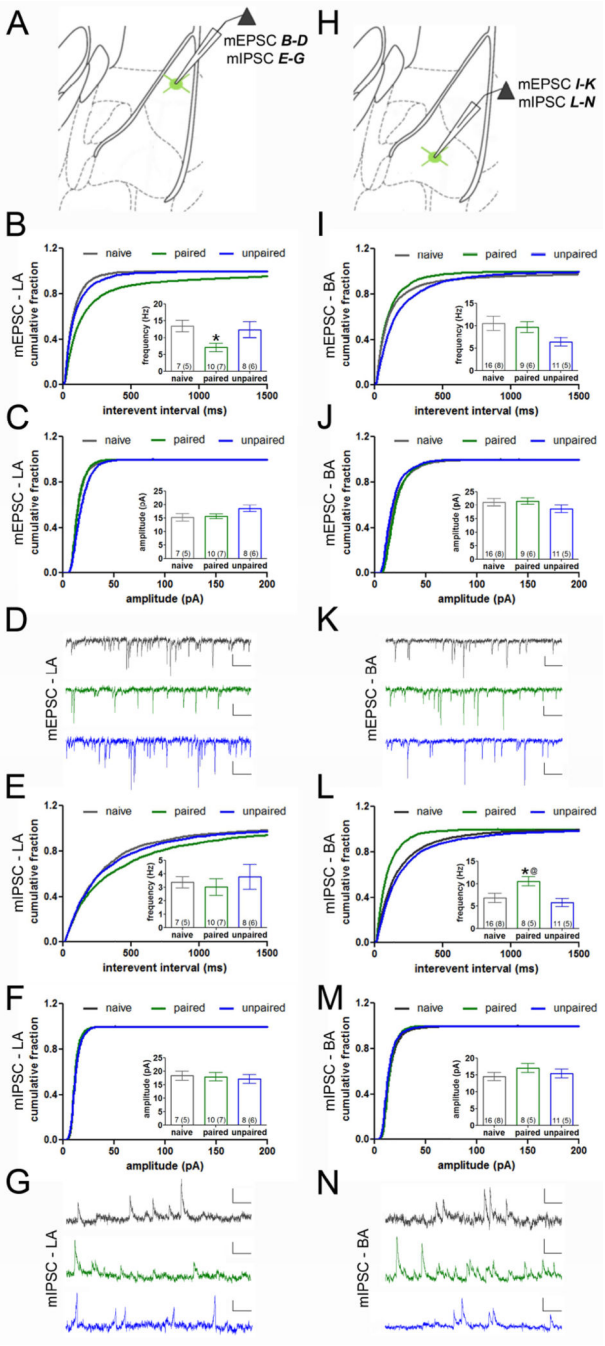

Figure 3. Auditory fear conditioning induces nucleus-specific remodeling of synaptic input onto PV-INs

Miniature postsynaptic currents were recorded in PV-INs with a low chloride internal solution, allowing for isolation of EPSCs and IPSCs at −60 mV and 0 mV, respectively. **A**. Schematic of LA miniature postsynaptic recordings in B–G. **B–D**. Frequency (**B**) but not amplitude (**C**) of mEPSCs (representative traces in **D**) was reduced in LA PV-INs of mice that received paired, but not unpaired, training as compared to naïve mice. **E–G**. The frequency (**E**) and amplitude (**F**) of mIPSCs was unaffected (representative traces in **G**). **H**.

Schematic of BA miniature postsynaptic recordings in I–N. **I–K**. The frequency (**I**) and amplitude (**J**) of mEPSCs (representative traces in **K**) in BA PV-INs were unaffected by training. **L–N**. The frequency (**L**) but not amplitude (**M**) of mIPSCs (representative traces in **N**) was increased after paired, but not unpaired, training compared to the naïve condition. Scales = D,G,K, 10 pA × 100 ms; N, 20 pA × 100 ms. n/group indicated on bar histograms. One-way ANOVA followed by Fisher's LSD, * $p < 0.05$ naïve versus paired, @ $p < 0.05$ paired versus unpaired. Data presented as mean ± SEM.

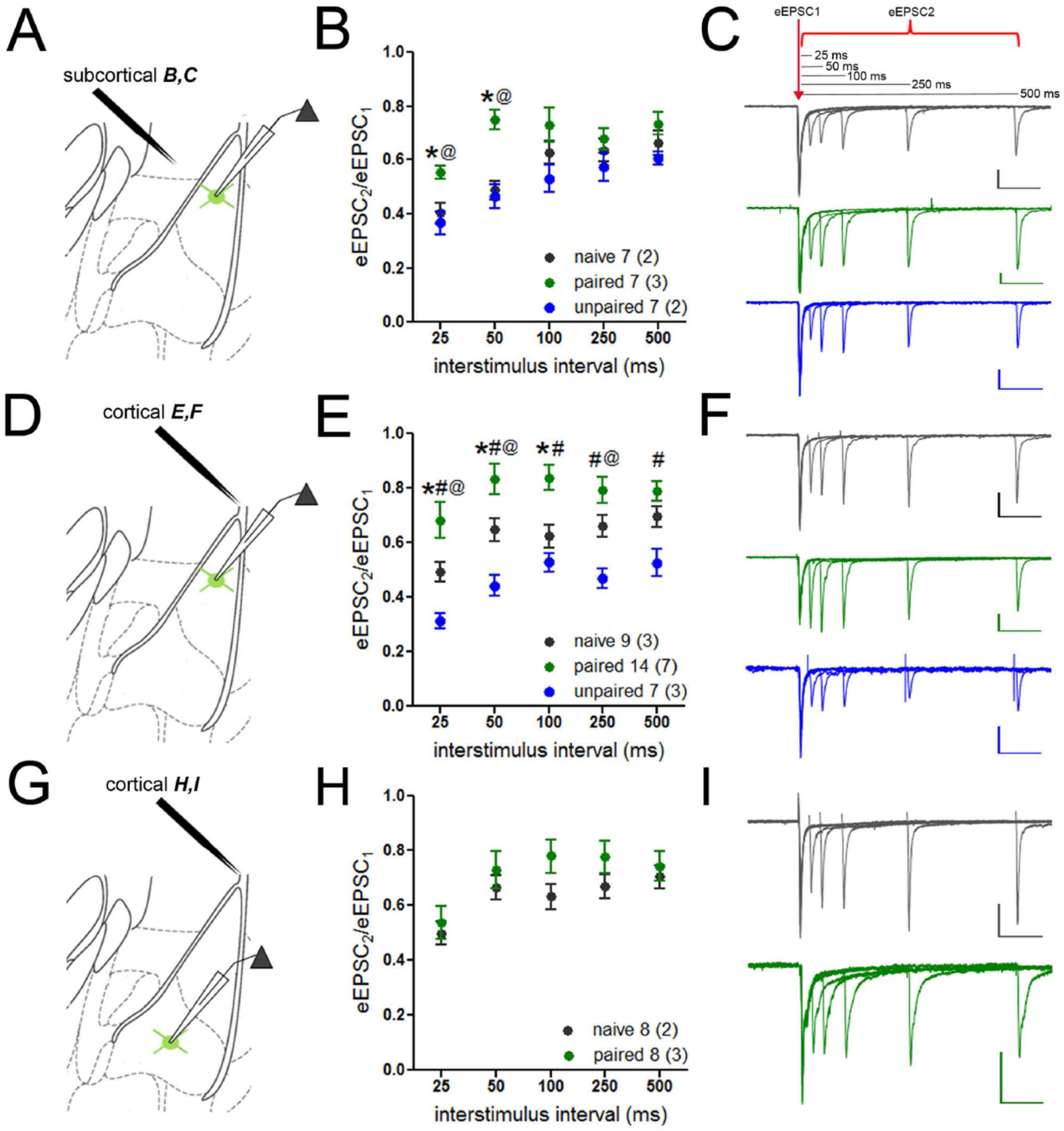

Figure 4. Reduced afferent input onto lateral, but not basal, amygdala PV-INs after fear memory encoding

Release probability of excitatory subcortical and cortical inputs to PV-INs was assayed by paired-pulse stimulation of the internal (**A**) and external capsules (**D,G**), respectively. **A–C**. Paired-pulse ratio (PPR; $EPSC_2/EPSC_1$) of subcortical EPSCs was increased in LA PV-INs from mice that received paired training compared to both unpaired and naïve conditions. Representative traces in **C. D–F**. PPR of cortical EPSCs was increased in LA PV-INs in mice that received paired training compared to both naïve and unpaired conditions.

Representative traces in **F. G–I**. PPR of cortical EPSCs was not altered by fear conditioning in BA PV-INs. Representative traces in **I**. Scales = 80 pA × 100 ms. n/group indicated on graphs. Repeated-measured ANOVA followed by Holm-Bonferroni, * $p < 0.05$ naïve versus paired, @ $p < 0.05$ paired versus unpaired, # $p < 0.05$ naïve versus unpaired. Data presented as mean ± SEM.

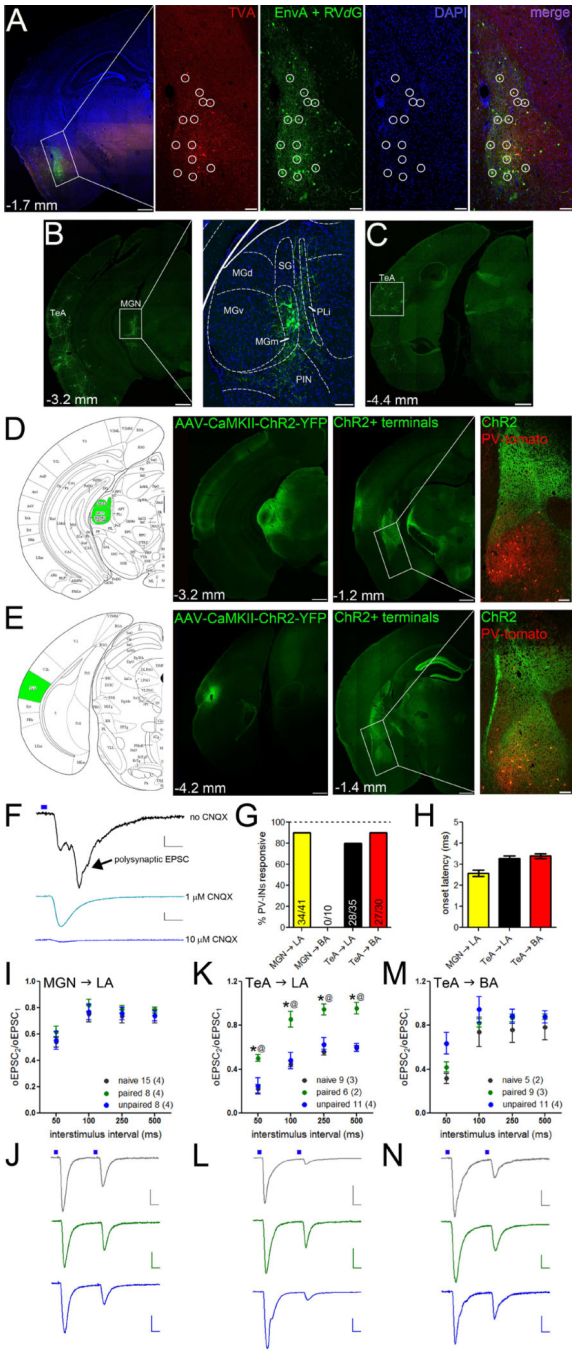

Figure 5. Presynaptic origins of internal and external capsule plasticity

A. AAV-FLEX-TVA-mCherry and the rabies glycoprotein was unilaterally injected into the basolateral amygdala of PV-IRES-Cre mice to restrict subsequent expression of EnvA +RV*d*G-eGFP to PV-INs and their monosynaptic retrograde partners. Confocal images of the injection site (boxed portion on left) are enlarged in the right panels. Retrograde labeling only occurred from PV-INs that coexpressed mCherry (red) and eGFP (green; circles). **B–C**. eGFP-positive cell bodies were observed in temporal association cortex (TeA; **B–C**) and the medial portion of the medial geniculate nucleus (MGN; **B**). The boxed portion of the MGN

on left is enlarged in the right panel. MG dorsal (d), ventral (v), and medial (m); suprageniculate nucleus (SG); posterior limitans nucleus (PLi); posterior intralaminar nucleus (PIN). **D–E**. AAV-CaMKII-ChR2-eYFP was injected into the MGN (**D**) and TeA (**E**) of PV-IRES-Cre mice crossed to ROSA-tdTomato reporter mice to target PV-INs for electrophysiological recordings without exciting ChR2. eYFP-positive terminal expression shown in right panels with the boxed portion representing the enlarged images of basolateral amygdala to the right. Scales = low magnification, 500 μm; enlargements, 100 μm. **F**. Optic-evoked EPSCs (oEPSCs) were conducted in the presence of 10 μM CPP and 1 μM CNQX to prevent polysynaptic activity and isolate monosynaptic currents. oEPSCs were abolished by saturating CNQX (10 μM). Scales = 10 pA × 10 ms. **G**. Terminal stimulation elicited oEPSCs from both pathways onto LA PV-INs; only TeA oEPSCs were observed in BA PV-INs. **H**. Onset latency of oEPSCs was consistent with monosynaptic transmission in both pathways. **I–J**. Fear learning did not alter PPR of oEPSCs at MGN → LA PV-IN synapses. Representative traces in **J. K–N**. PPR of oEPSCs at TeA → PV-IN synapses was increased in paired compared to unpaired and naïve mice in LA (**K**, representative traces in **L**) but not BA (**M**, representative traces in **N**). J,L,N representative traces shown at the 50 ms interstimulus interval. Scales J,L,N = 10 pA × 50 ms. n/group indicated on graphs. I,K,M repeated-measured ANOVA followed by Holm-Bonferroni. Data presented as mean ± SEM.

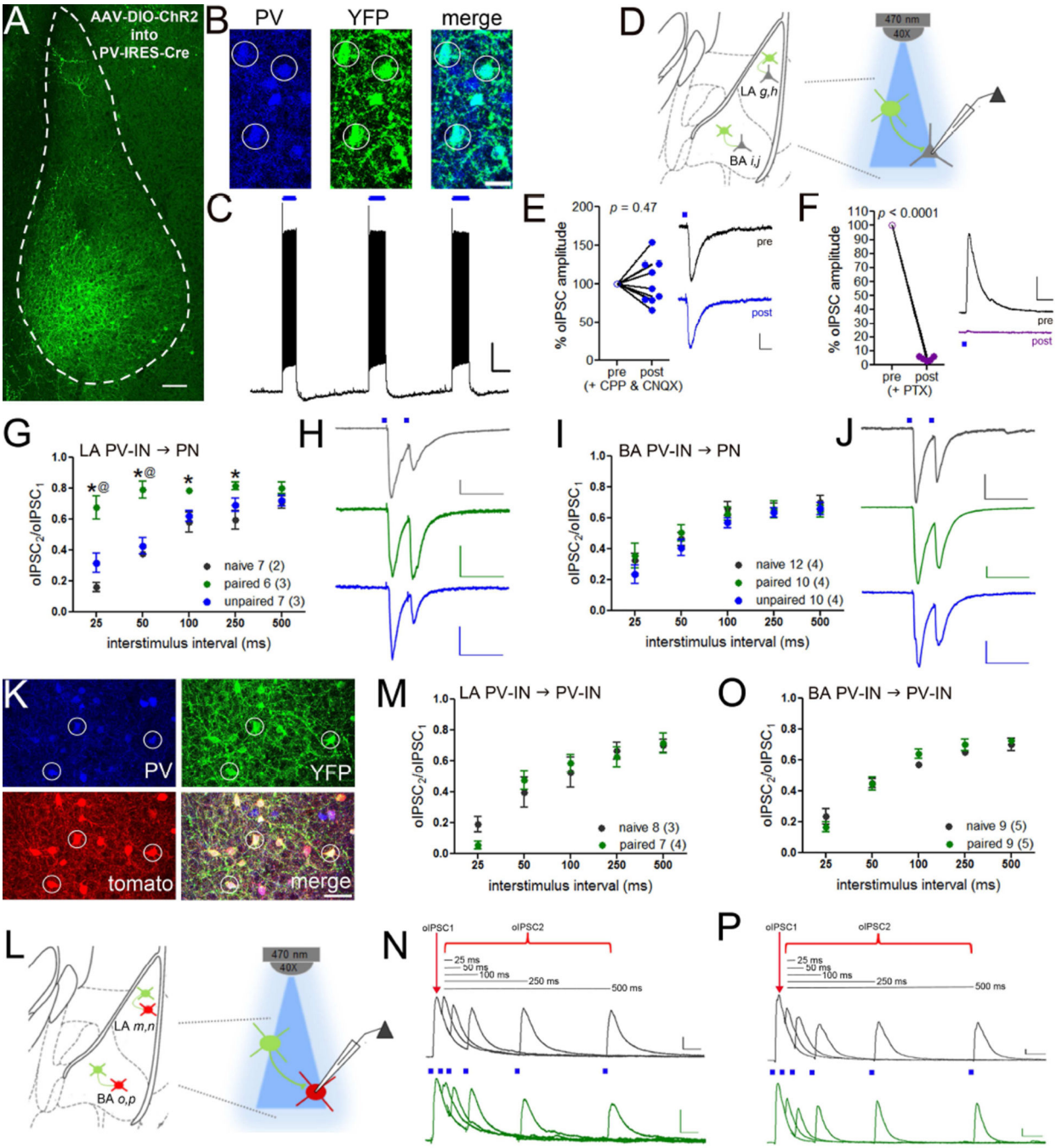

Figure 6. Nucleus- and target-specific reduction in GABA release from PV-INs after auditory fear conditioning

A. AAV-DIO-ChR2-eYFP was injected into the basolateral amygdala of PV-IRES-Cre mice for optogenetic-assisted *in vitro* slice electrophysiology, scale = 100 μm. **B**. Immunofluorescence staining confirmed that eYFP (green) was exclusively expressed in PV-positive neurons (blue), scale = 25 μm. **C**. Blue light (λ= 470 nm) evoked action potential generation in ChR2+ PV-INs. Scale = 15 mV × 1 s. **D**. Recording configuration in E–H. Release probability at PV-IN → principal neuron (PN) synapses was assayed by paired-

pulse optic stimulation (λ= 470 nm) in LA (G–H) and BA (I–J). **D–E**. Light-evoked currents were unaffected by the glutamate receptor antagonists APV and CNQX (**E**, scale = 20 pA × 25 ms) and abolished by PTX (**F**, scale = 100 pA × 50 ms). **G**. Paired pulse ratio (PPR) of PV-IN → PN IPSCs in LA was increased in mice that received paired training compared to unpaired and naïve conditions. Representative traces in **H. I**. PPRs were unaltered in BA. Representative traces in **J**. Representative traces are shown at the 50 ms interstimulus interval. Scales = H, 50 pA × 100 ms; J, 60 pA × 100 ms. **K**. AAV-DIO-ChR2-eYFP was injected into the basolateral amygdala of PV-IRES-Cre mice crossed to ROSA-tdTomato reporter mice to target PV-INs for electrophysiological recordings without gating ChR2. **L**. Schematic of O–R. Release probability at PV-IN → PV-IN synapses was assayed by paired-pulse optical stimulation (λ = 470 nm) during recording from tdTomato-positive PV-INs in LA (M–N) and BA (O–P). **M–P**. PPR of PV-IN → PV-IN IPSCs was unaffected by training in the LA (**M**, representative traces in **N**) and BA (**O**, representative traces in **P**). IPSC recordings were conducted at 0 mV in order to exclude postsynaptic ChR2 currents based on their ionic reversal. Scales = N,P 50 pA × 50 ms. n/group indicated on graphs. E,F paired samples t-test; G,I,M,O repeated measured ANOVA followed by planned comparisons with Holm-Bonferroni. * $p < 0.05$ naïve versus paired, @ $p < 0.05$ paired versus unpaired. Data presented as mean ± SEM.

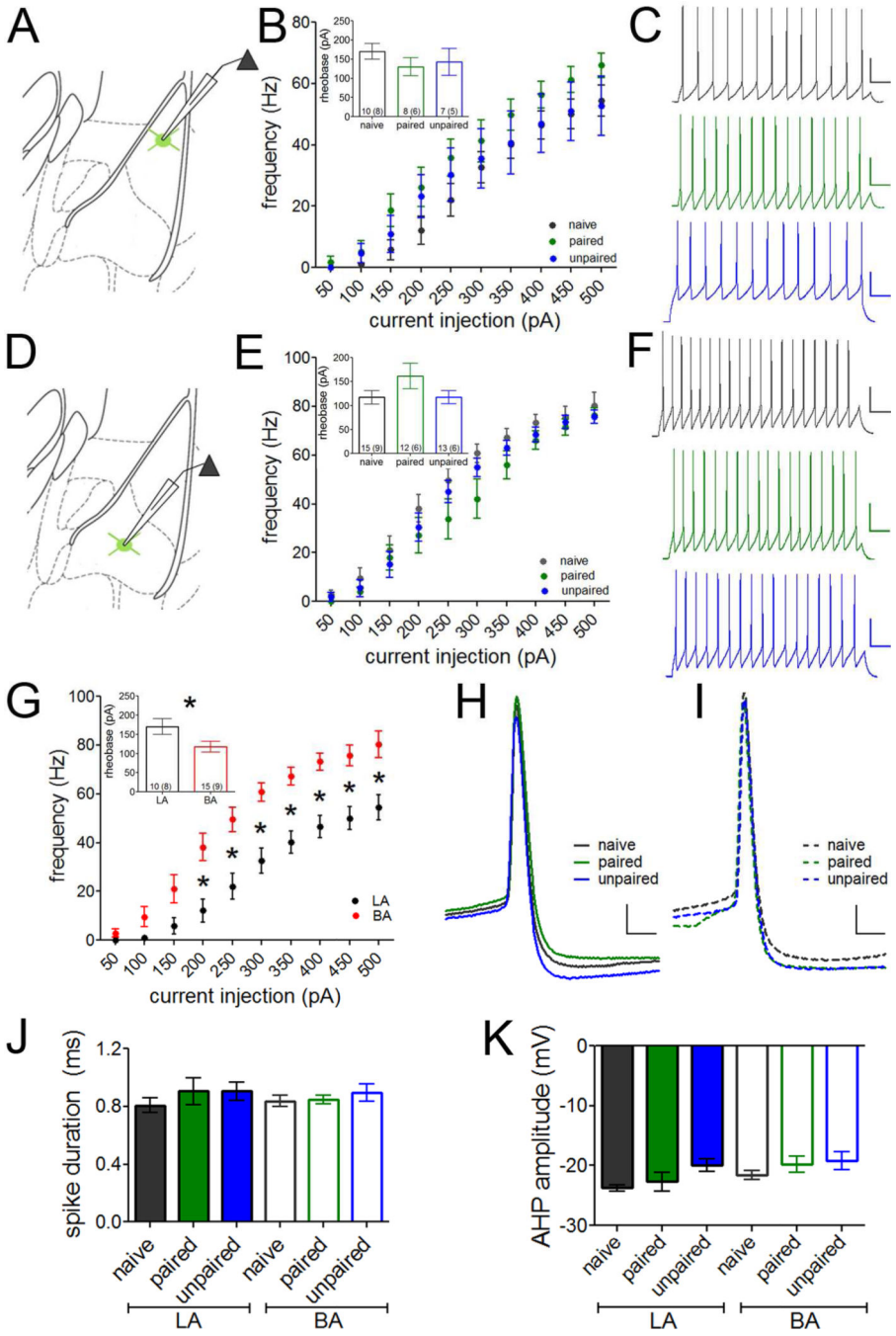

Figure 7. Fear memory encoding does not affect PV-IN intrinsic excitability

Action potentials were elicited in PV-INs in LA (A–C) and BA (D–F) by somatic current injections of increasing amplitude. **A**. Recording configuration in B–C. No differences in intrinsic excitability were observed among groups in LA PV-INs (**B**, representative traces at the 200 pA current injection in **C**). **D**. Recording configuration in E–F. No differences in intrinsic excitability were observed among groups in BA PV-INs (**E**, representative traces at the 200 pA current injection in **F**). Scales = 50 pA × 25 ms. **G**. In naïve animals, PV-INs in LA were less excitable than PV-INs in BA, requiring more current to fire a single action

potential (rheobase current; inset) and firing fewer action potentials to current injections greater than 150 pA. **H–K**. Individual spike characteristics were quantified in LA (**H**) and BA (**I**) at rheobase. Overlays of representative traces are shown. Scales = 10 pA × 2 ms. No differences were observed among groups or between nuclei in any spike parameter, including spike duration (**J**) and after hyperpolarization (AHP) amplitude (**K**). n/group indicated on graphs. G, repeated-measures ANOVA following by Holm-Bonferroni or independent samples t-test (inset). * $p < 0.05$. Data presented as mean ± SEM.